Meteoritics & Planetary Science 41, Nr 7, 1081–1094 (2006)
Abstract available online at http://meteoritics.org

Terrestrial ages, pairing, and concentration mechanism of Antarctic chondrites from Frontier Mountain, Northern Victoria Land

K. C. WELTEN[1†*], K. NISHIIZUMI[1], M. W. CAFFEE[2] , D. J. HILLEGONDS[2], J. A. JOHNSON[3], A. J. T. JULL[3], R. WIELER[4], and L. FOLCO[5]

[1]Space Sciences Laboratory, University of California–Berkeley, Berkeley, California 94720–7450, USA
[2]Center for Accelerator Mass Spectrometry, Lawrence Livermore National Laboratory, Livermore, California 94550, USA
[3]NSF-Arizona Accelerator Mass Spectrometry Facility, The University of Arizona, Tucson, Arizona 85721, USA
[4]ETH Zürich, Isotope Geology and Mineral Resources, NO C61, CH-8092 Zürich, Switzerland
[5]Museo Nazionale dell'Antartide, Università di Siena, Via Laterina 8, I-53100 Siena, Italy
[†]Department of Physics, Purdue University, West Lafayette, Indiana 47907, USA
[*]Corresponding author. E-mail: kcwelten@berkeley.edu

(Received 25 June 2005; revision accepted 24 April 2006)

Abstract–We report concentrations of cosmogenic ^{10}Be, ^{26}Al, ^{36}Cl, and ^{41}Ca in the metal phase of 26 ordinary chondrites from Frontier Mountain (FRO), Antarctica, as well as cosmogenic ^{14}C in eight and noble gases in four bulk samples. Thirteen out of 14 selected H chondrites belong to two previously identified pairing groups, FRO 90001 and FRO 90174, with terrestrial ages of ~40 and ~100 kyr, respectively. The FRO 90174 shower is a heterogeneous H3-6 chondrite breccia that probably includes more than 300 individual fragments, explaining the high H/L chondrite ratio (3.8) at Frontier Mountain. The geographic distribution of 19 fragments of this shower constrains ice fluctuations over the past 50–100 kyr to less than ~40 m, supporting the stability of the meteorite trap over the last glacial cycle. The second H-chondrite pairing group, FRO 90001, is much smaller and its geographic distribution is mainly controlled by wind-transport. Most L-chondrites are younger than 50 kyr, except for the FRO 93009/01172 pair, which has a terrestrial age of ~500 kyr. These two old L chondrites represent the only surviving members of a large shower with a similar preatmospheric radius (~80 cm) as the FRO 90174 shower. The find locations of these two paired L-chondrite fragments on opposite sides of Frontier Mountain confirm the general glaciological model in which the two ice flows passing both ends of the mountain are derived from the same source area on the plateau. The 50 FRO meteorites analyzed so far represent 21 different falls. The terrestrial ages range from 6 kyr to 500 kyr, supporting the earlier proposed concentration mechanism.

INTRODUCTION

In the past three decades more than 25,000 meteorite specimens have been found in Antarctica. Most of these meteorites were concentrated on blue ice regions, which are found in the vicinity of the Transantarctic Mountains on one side and the Yamato and Sør Rondane Mountains on the other side of the continent. One of these so-called stranding areas is located near Frontier Mountain (FRO), in northern Victoria Land (~73°S, 160°30′E). After the chance discovery of 37 meteorites in 1984 (Delisle et al. 1989), EUROMET visited this area in 1990, and recovered another ~230 meteorites (Delisle et al. 1993; Folco and Bland 1994). Radio echo sounding measurements, meteorite find locations, and other field observations during the 1984 and 1990 seasons clarified to a large degree the concentration mechanism operating at FRO (Delisle et al. 1989; Cassidy et al. 1992; Delisle et al. 1993). In four more expeditions between 1993–1999, yielding another 205 meteorites, extensive studies were carried out to measure bedrock topography, ice thickness, ice-flow rates, and ice ablation rates. These studies verified the mechanism proposed previously and resulted in a more quantitative description of the FRO meteorite trap. Based on the combined studies, a model of the local glaciology and meteorite concentration mechanism was proposed as described in Folco et al. (2002).

Frontier Mountain (72°59′S, 160°20′E) is a ridge 9 km in length at the edge of the East Antarctic plateau. With a highest peak of 2804 m above sea level, this ridge forms a barrier for ice flowing from the Polar Plateau (at ~2310 m above sea

level) to the Rennick Glacier, which eventually drains into the southern Pacific Ocean. The polar ice flows around both ends of Frontier Mountain in a general northeastern direction. Part of the ice flow passing the south end of FRO bends off to the north and is slowed down (due to a submerged barrier) from horizontal velocities of >1 m/yr to <0.1 m/yr. In this area, strong katabatic winds prevent snow accumulation and expose a ~42 km^2 blue ice field to active ablation with an average rate of ~6 cm/yr. This blue ice field has yielded more than 700 meteorites so far. The meteorite trap consists of three main collection sites, the "Meteorite Valley moraine," the "scatter field," and the "firn-ice edge" (Fig. 1).

In a previous study we measured the noble gases and cosmogenic radionuclides in 26 H chondrites and one L chondrite from the FRO collection to determine their terrestrial ages and exposure ages (Welten et al. 1999). We found terrestrial ages up to ~200 kyr and concluded that about half of these samples were part of two H5/6-chondrite showers, FRO 90001 (4 members) and FRO 90174 (7–9 members). In a follow-up study we determined that the FRO 90174 shower (Welten et al. 2001) had a preatmospheric radius, R, of 80–100 cm, whereas the object that produced the FRO 90001 shower was much smaller (R < 30 cm). In an effort to understand the concentration mechanism of the Frontier Mountain "meteorite trap," we selected 23 additional meteorites from this area for terrestrial age determination. In addition we selected three recently discovered meteorites from nearby ice fields, Johannesen Nunataks (JOH), Miller Butte (MIB), and Mount Walton (WAL). These ice fields are less than ~40 km from FRO and represent the same large-scale drainage area, i.e., the southeastern sector of Talos Dome.

In this work we present concentrations of cosmogenic ^{10}Be (half-life = 1.5 × 10^6 yr), ^{26}Al (7.05 × 10^5 yr), ^{36}Cl (3.01 × 10^5 yr) and ^{41}Ca (1.04 × 10^5 yr) in the metal fraction of 26 ordinary chondrites, as well as concentrations of cosmogenic ^{14}C in eight bulk samples and noble gases in four samples. We determined the terrestrial ages of these meteorites and further evaluated the extent of pairing, especially among H chondrites (Welten et al. 1999; 2001). We discuss the implications of the terrestrial ages and pairing of these meteorites in terms of the meteorite concentration mechanism and past ice fluctuations at Frontier Mountain.

EXPERIMENTAL METHODS

Sample Selection

We carefully selected 23 ordinary chondrites from the FRO collection based on petrologic type, location of find, and degree of weathering (Table 1). The nine L chondrites include a few of each petrologic type (3–6), whereas for the H chondrites we selected relatively more type 3 and 4 chondrites in an attempt to avoid specimens of the two main H-chondrite showers (FRO 90001 and FRO 90174). The selection includes specimens from the three main collection sites, known as the Meteorite Valley (MV), the scatter field (SF), and the firn-ice edge (FIE). Five H chondrites from Meteorite Valley were selected, because they may be older than others found in this area: FRO 01022, 01023, and 01152 were found in a morainic deposit up to 50 m above the local ice level in Meteorite Valley, whereas FRO 01044 and 01049 were found at the terminal front of Meteorite Valley (Fig. 1). Of the seven selected meteorites from the scatter field, five are larger than the threshold of 200 g for wind transport. These meteorites were probably not affected by wind-driven transport (Folco et al. 2002). Assuming that some of these meteorites were released from the ablating ice relatively recently (in the last 10 kyr), their terrestrial ages may constrain the formation age of the ice. Two L chondrites, FRO 93009 (L4) from Meteorite Valley and FRO 01172 (L3) from the Central Moraine (CM) (Fig. 1) were selected in particular, because they are macroscopically very weathered, which could indicate very long terrestrial ages. Finally, JOH 01001, MIB 01001, and WAL 01001 were selected because they were recently found (December 2001) on blue ice areas close to Frontier Mountain (Ferraris et al. 2003).

^{14}C Measurements

For eight samples we measured concentrations of cosmogenic ^{14}C. Samples were crushed to a powder and treated with 100% phosphoric acid to remove carbonates, which formed during terrestrial weathering. After the residues were washed with distilled water and dried, aliquots ranging in size from 53–272 mg were mixed with ~5 g of iron chips and placed in an alumina crucible. The crucible was placed in an oven at 500 °C to remove most low-temperature contaminants. The sample was heated in a RF induction furnace to 1400 °C in a flow of oxygen and all carbonaceous gases were converted to CO_2. The volume of CO_2 was measured to monitor for possible leaks and to determine the carbon contents of the samples. The measured carbon contents are generally <1 mg/g, whereas the L3 chondrite FRO 99031 shows a significantly higher value of 1.8 mgC/g (Table 4). These carbon results are consistent with trends of decreasing carbon content as a function of petrologic type for ordinary chondrites falls (Makjanic et al. 1993). The CO_2 was converted to graphite, of which the $^{14}C/C$ ratio was measured at the NSF-Arizona AMS facility together with blanks and NIST oxalic-I and II standards (Donahue et al. 1990). The measured ratio was first corrected for background and normalized to 1950 A.D. carbon ($^{14}C/C = 1.177 \times 10^{-12}$), and then corrected for an extraction background of (1.25 ± 0.30) × 10^6 atoms ^{14}C, following the procedure of Jull et al. (1993). The corrected ^{14}C concentrations (in dpm/kg) are reported in Table 2.

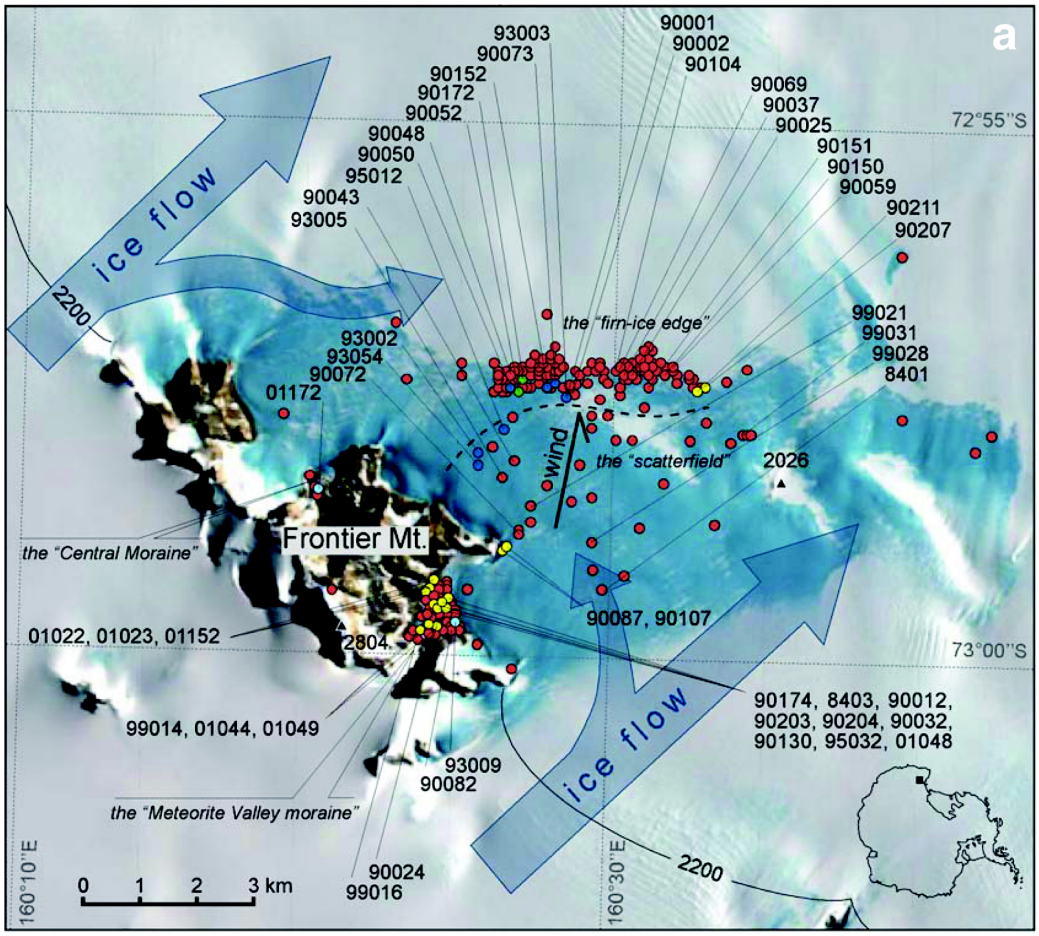

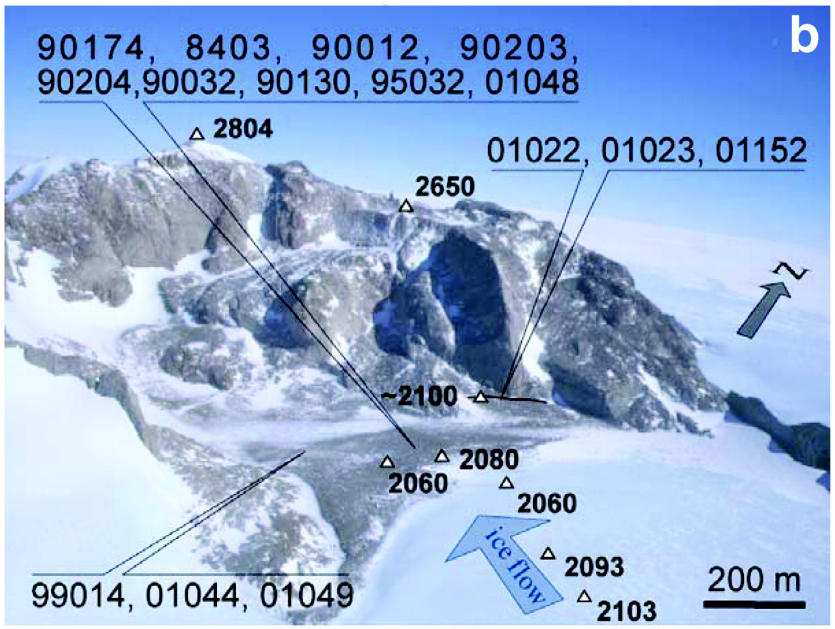

Fig. 1. a) A schematic map of the Frontier Mountain blue ice field showing the geographic distribution of the FRO 90174 shower (yellow dots), the FRO 90001 pairing group (blue dots), and the FRO 93009/01172 pair (cyan dots) relative to other FRO meteorites (red dots) studied in this work. Meteorites studied by Welten et al. (1999, 2001) are labeled in black. b) A panoramic view of the Meteorite Valley moraine from the southeast. The geographic distribution of the FRO 90174 paired fragments in the area is shown. The black line marks the limit of the moraine attained during a former, ~40 m higher stand of the ice, as indicated by the find locations of FRO 01022, 01023, and 01152.

Table 1. Classification and location of ordinary chondrite finds from Frontier Mountain (FRO) and surrounding ice fields (Johannesen Nunataks, JOH; Miller Butte, MIB; Mount Walton, WAL). Also shown are the bulk metal content of each meteorite (in wt%), the amount of purified metal (in mg) dissolved for radionuclide analysis as well as the concentrations of Ni, Co, and Mg (in wt%) in the metal fraction, as measured by atomic absorption spectrometry. The last column shows the amount of silicate contamination, estimated from the measured Mg concentration, assuming an average Mg concentration of 17 wt% in chondritic silicates.

Meteorite	Mass (g)	Type	Shock[a] /WG[b]	Location of find[c]	% metal	Dissolved metal	Ni	Co	Mg	Silicate
H chondrites										
FRO 90032	1.6	H3	–	MV	9.0	84.6	9.3	0.49	0.051	0.30
FRO 90130	15.5	H3-5	–	MV	8.9	95.1	9.1	0.51	0.044	0.26
FRO 93002	665.2	H6	S3/B	SF	12.2	95.1	9.6	0.51	0.006	0.03
FRO 93054	1438.0	H6	B	SF	13.6	88.1	9.2	0.50	0.006	0.04
FRO 95012	44.0	H6	A	SF	11.7	90.1	9.4	0.50	0.009	0.05
FRO 95032	17.4	H4	S3/W1	MV	9.4	85.3	10.3	0.45	0.078	0.46
FRO 99014	14.1	H4	S2/W2	MV	10.8	102.1	8.6	0.58	0.072	0.42
FRO 99021	127.9	H4	S1/W1	SF	18.7	100.2	10.3	0.49	0.178	1.05
FRO 01022	3.5	H5	S2/W2	MV	10.6	80.6	9.7	0.58	0.062	0.37
FRO 01023	3.3	H6	S2/W2	MV	6.9	62.5	9.7	0.59	0.018	0.11
FRO 01044	26.6	H5	S2/W2	MV	10.8	82.3	9.9	0.58	0.058	0.34
FRO 01048	6.8	H3/4	S2/W1-2	MV	7.9	52.5	10.5	0.59	0.017	0.10
FRO 01049	44.1	H3/4	S1/W1-2	MV	8.7	80.1	11.8	0.58	0.061	0.36
FRO 01149	1.5	H4	S1/W4	FRO	0.0	N/A	N/A	N/A	N/A	N/A
FRO 01152	1.5	H4	S2/W2	MV	5.2	47.5	10.6	0.56	0.053	0.31
JOH 01001	1058.7	H5	S1/W2	JOH	14.1	82.0	11.7	0.61	0.017	0.10
WAL 01001	271.6	H4/5	S2/W2	WAL	11.5	82.4	10.0	0.55	0.081	0.47
L chondrites										
FRO 90052	34.2	L4	–	FIE	5.5	51.2	20.5	0.95	0.101	0.59
FRO 90172	65.9	L5	–	FIE	3.7	39.4	21.4	0.92	0.058	0.34
FRO 93003	65.3	L6	S3/A	FIE	7.6	81.2	16.1	0.70	0.022	0.13
FRO 93005	1665.4	L5	S3/A	SF	6.5	76.1	17.8	0.67	0.040	0.24
FRO 93009	106.5	L4	W2	MV	4.5	64.3	14.3	0.69	0.030	0.18
FRO 99016	23.3	L5	S2/W1	MV	4.3	43.3	10.2	0.97	0.047	0.28
FRO 99028	771.8	L6	S4/W1	SF	6.8	89.3	16.9	0.69	0.167	0.98
FRO 99031	201.6	L3	S4/W1	SF	5.5	84.8	17.2	0.60	0.033	0.19
FRO 01172	150.2	L3	S3/W2	CM	4.5	75.3	13.9	0.75	0.035	0.20
MIB 01001	6260.0	L5	S3/W1	MIB	5.3	67.7	17.0	0.74	0.141	0.83

[a]Shock after Stöffler et al. (1991).
[b]Weathering grade: A = minor rustiness, B = moderate rustiness; W1–W6 after Wlotzka (1993).
[c]MV = Meteorite Valley moraine; SF = scatter field; FIE = firn-ice edge, FRO = Frontier Mountain bedrock, and CM = Central moraine. For further details, see Fig. 1a and Folco et al. (2002).

Table 2. Terrestrial ages of FRO meteorites based on measured concentrations of cosmogenic ^{14}C and saturation values of 46 ± 7 dpm/kg for H chondrites and 51 ± 8 dpm/kg for L chondrites. The measured amounts of ^{14}C (column 7) are corrected for an extraction background of (1.21 ± 0.30) × 10^6 atoms to determine the cosmogenic ^{14}C concentration (column 8).

Meteorite	Type	Weight (g)	CO_2 (cm^3)	C (mg/g)	$^{14}C/C$ ratio ($\times 10^{12}$)	^{14}C atoms ($\times 10^6$)	^{14}C dpm/kg	^{14}C-age (kyr)
FRO 8401	L6	–	–	–	–		10.4 ± 1.2	13 ± 2
FRO 90052	L4	0.097	0.180	0.91	0.576 ± 0.010	2.55 ± 0.05	3.2 ± 0.7	23 ± 2
FRO 90072	H5	0.148	0.120	0.40	0.606 ± 0.013	1.79 ± 0.04	0.9 ± 0.5	32 ± 4
FRO 93003	L6	0.070	0.090	0.63	0.522 ± 0.018	1.16 ± 0.04	−0.2 ± 1.0	>34
FRO 93005	L5	0.272	0.060	0.11	2.297 ± 0.042	3.39 ± 0.06	1.8 ± 0.3	27 ± 2
FRO 99016	L5	0.177	0.074	0.21	0.635 ± 0.018	1.16 ± 0.03	−0.1 ± 0.4	>40
FRO 99021	H4	0.147	0.074	0.25	0.500 ± 0.019	0.91 ± 0.04	−0.5 ± 0.5	>40
FRO 99028	L6	0.053	0.067	0.62	1.321 ± 0.021	2.18 ± 0.04	4.2 ± 1.3	21 ± 3
FRO 99031	L3	0.118	0.440	1.83	1.300 ± 0.012	14.08 ± 0.13	25.1 ± 0.6	6 ± 1

Table 3. Concentrations of cosmogenic radionuclides (in dpm/kg) in the metal fraction of ordinary chondrites from Frontier Mountain and nearby ice fields. Errors (1σ) include uncertainties in the AMS measurements of samples, blanks, and standards, but not those in the absolute value of the standards. Terrestrial ages (in kyr) were calculated from the obtained radionuclide results.

FRO	^{10}Be	^{26}Al	^{36}Cl	^{41}Ca	^{26}Al/^{10}Be	^{36}Cl/^{10}Be	^{41}Ca/^{36}Cl	T (terr)	Method[a]
H chondrites									
FRO 90032[b]	3.21 ± 0.07	2.45 ± 0.12	14.3 ± 0.3	9.2 ± 0.8	0.76 ± 0.04	4.46 ± 0.13	0.64 ± 0.06	103 ± 26	2, 3
FRO 90130[b]	2.82 ± 0.06	2.10 ± 0.05	13.6 ± 0.3	9.4 ± 0.5	0.74 ± 0.03	4.84 ± 0.14	0.69 ± 0.04	94 ± 33	2, 3
FRO 93002[c]	3.67 ± 0.07	3.04 ± 0.07	21.1 ± 0.5	18.3 ± 1.0	0.83 ± 0.04	5.76 ± 0.19	0.87 ± 0.05	40 ± 20	4
FRO 93054[c]	3.51 ± 0.07	2.78 ± 0.07	20.8 ± 0.4	20.4 ± 1.1	0.79 ± 0.06	5.93 ± 0.17	0.98 ± 0.05	24 ± 20	4
FRO 95012[c]	3.35 ± 0.07	2.85 ± 0.08	21.3 ± 0.4	20.7 ± 1.1	0.85 ± 0.03	6.35 ± 0.18	0.97 ± 0.06	22 ± 20	4
FRO 95032[b]	2.88 ± 0.06	2.06 ± 0.07	13.7 ± 0.3	9.5 ± 0.5	0.72 ± 0.03	4.75 ± 0.13	0.70 ± 0.04	94 ± 28	2, 3
FRO 99014[b]	3.42 ± 0.07	2.39 ± 0.07	14.2 ± 0.3	10.0 ± 0.5	0.70 ± 0.03	4.17 ± 0.12	0.70 ± 0.04	106 ± 18	2, 3
FRO 99021	5.20 ± 0.10	3.84 ± 0.17	22.3 ± 0.5	19.6 ± 1.8	0.74 ± 0.04	4.28 ± 0.12	0.88 ± 0.04	43 ± 15	1, 3
FRO 01022[b]	2.65 ± 0.06	1.89 ± 0.06	12.4 ± 0.3	8.5 ± 0.6	0.71 ± 0.03	4.66 ± 0.13	0.69 ± 0.05	100 ± 25	2, 3
FRO 01023[b]	3.29 ± 0.07	2.39 ± 0.06	14.9 ± 0.3	10.0 ± 0.8	0.74 ± 0.03	4.52 ± 0.13	0.67 ± 0.06	92 ± 25	2, 3
FRO 01044[b]	3.19 ± 0.06	2.34 ± 0.06	14.6 ± 0.3	9.2 ± 0.5	0.75 ± 0.03	4.57 ± 0.13	0.63 ± 0.04	109 ± 33	2, 3
FRO 01048[b]	3.65 ± 0.07	2.52 ± 0.06	15.5 ± 0.3	9.7 ± 0.5	0.70 ± 0.03	4.25 ± 0.12	0.62 ± 0.04	113 ± 23	2, 3
FRO 01049[b]	3.32 ± 0.07	2.59 ± 0.06	14.9 ± 0.3	9.4 ± 0.5	0.80 ± 0.03	4.48 ± 0.13	0.63 ± 0.04	108 ± 30	2, 3
FRO 01152[b]	3.36±0.07	2.27 ± 0.06	14.5 ± 0.3	9.3 ± 0.7	0.69 ± 0.03	4.31 ± 0.12	0.64 ± 0.05	112 ± 20	2, 3
JOH 01001	5.86 ± 0.12	4.13 ± 0.10	–	22.4 ± 1.1	0.70 ± 0.02	–	–	11 ± 20	4
WAL 01001	5.23 ± 0.11	4.02 ± 0.13	–	19.7 ± 0.9	0.77 ± 0.03	–	–	30 ± 20	4
L chondrites									
FRO 90052[d]	4.72 ± 0.10	3.95 ± 0.12	26.4 ± 0.5	18.4 ± 0.8	0.84 ± 0.03	5.59 ± 0.16	0.70 ± 0.03	23 ± 2	1
FRO 90172[d]	4.75 ± 0.12	3.90 ± 0.10	26.9 ± 0.5	20.3 ± 1.2	0.82 ± 0.03	5.66 ± 0.18	0.75 ± 0.05	23 ± 2	1
FRO 93003	4.77 ± 0.10	3.96 ± 0.08	21.4 ± 0.4	18.4 ± 0.7	0.83 ± 0.02	4.48 ± 0.13	0.86 ± 0.04	45 ± 10	1, 3
FRO 93005	5.62 ± 0.11	4.42 ± 0.12	23.5 ± 0.5	21.4 ± 1.1	0.79 ± 0.03	4.18 ± 0.12	0.91 ± 0.05	27 ± 2	1
FRO 93009[e]	2.79 ± 0.07	1.58 ± 0.07	5.6 ± 0.1	0.64 ± 0.23	0.57 ± 0.03	2.02 ± 0.06	0.11 ± 0.04	480 ± 24	2, 3
FRO 99016	5.52±0.11	4.13 ± 0.10	23.6 ± 0.5	18.7 ± 1.4	0.75 ± 0.02	4.29 ± 0.12	0.79 ± 0.06	45 ± 10	1, 3
FRO 99028	5.39 ± 0.11	4.28 ± 0.18	23.4 ± 0.5	23.2 ± 0.9	0.79 ± 0.04	4.34 ± 0.14	0.99 ± 0.04	21 ± 3	1
FRO 99031	4.00 ± 0.08	3.96 ± 0.08	23.8 ± 0.5	24.6 ± 0.8	0.99 ± 0.03	5.95 ± 0.17	1.03 ± 0.04	6 ± 1	1
FRO 01172[e]	3.21 ± 0.06	1.82 ± 0.06	5.8 ± 0.3	0.46 ± 0.13	0.57 ± 0.02	1.79 ± 0.05	0.08 ± 0.02	525 ± 25	2, 3
MIB 01001	5.73 ± 0.12	4.09 ± 0.16	–	19.3 ± 1.6	0.71 ± 0.03	–	–	33 ± 20	4

[a]Terr. age methods: 1 = ^{14}C; 2 = ^{36}Cl/^{10}Be, 3 = ^{41}Ca/^{36}Cl, 4 = ^{41}Ca

[b]Paired with FRO 90174.

[c]Paired with FRO 90001.

[d, e]Pairs.

Long-Lived Radionuclides

After crushing samples of 1.5–2.5 g in an agate mortar, we separated the metal fraction with a magnet. The magnetic fraction was cleaned in an ultrasonic bath with 0.2N HCl (10–30 min) to remove troilite, and then with concentrated HF (10–20 min) to remove attached silicates. The amount of clean metal separated from each FRO sample ranges from 5–19 wt% for H chondrites and 3.7–7.6 wt% for L chondrites (Table 1). One H chondrite, FRO 01149, did not contain any metal, which is consistent with its high degree of weathering, W4 according to the scale of Wlotzka (1993).

A carrier solution containing ~2 mg of Be, Al, and Ca and ~5 mg of Cl was added to the purified metal samples, which are typically between 40–100 mg. The samples are dissolved in 20 ml 1.5 N HNO_3 in an ultrasonic bath at ~50 °C. After complete dissolution of the samples, small aliquots were taken for chemical analysis by atomic absorption spectrometry (AAS), and Cl was separated as AgCl. From the remaining solution, Be, Al, and Ca were separated and purified as described previously (Welten et al. 1999). Concentrations of ^{10}Be, ^{26}Al, ^{36}Cl, and ^{41}Ca were measured by accelerator mass spectrometry (AMS) at LLNL (Davis et al. 1990). The measured ^{10}Be/Be, ^{26}Al/Al, ^{36}Cl/Cl, and ^{41}Ca/Ca ratios were corrected for blanks and normalized to AMS standards described elsewhere (Nishiizumi et al. 1984, 2000; Nishiizumi 2004, Sharma et al. 1990). The measured concentrations of ^{10}Be and ^{26}Al were corrected for small contributions of ^{10}Be and ^{26}Al from silicates. The amount of silicate contamination—estimated from the measured concentration of Mg in the metal—is generally <0.5 wt%, although a few metal samples (FRO 90052, 99021, 99028, and MIB 01001) contain 0.6–1.1 wt% silicates (Table 1). The final results (in dpm/kg) are listed in Table 3.

Table 4. Concentrations of Ca, Fe, Ni (in wt%) and of cosmogenic ^{10}Be, ^{26}Al, and ^{36}Cl (in dpm/kg) in the stone fraction of the paired L chondrites FRO 93009 and 01172. The last three columns give the concentrations of ^{10}Be, ^{26}Al, and ^{36}Cl at the time of fall (0), after correction of the measured concentrations for radioactive decay during the terrestrial residence time of 500 kyr. The ^{10}Be and ^{26}Al concentrations were also corrected for dilution of the stone fraction by oxidized metal (%Mox), while the ^{36}Cl concentrations were normalized to Fe+8Ca+16K.

FRO	Type	Ca	Fe	Ni	%Mox	^{10}Be	^{26}Al	^{36}Cl	^{10}Be(0)	^{26}Al(0)	^{36}Cl(0)
93009	L4	1.28	18.2	0.72	3.7	16.9 ± 0.3	40.6 ± 1.1	5.17 ± 0.14	22.5 ± 0.5	70.7 ± 2.0	59 ± 2
01172	L3	1.31	17.5	0.80	2.9	15.2 ± 0.3	35.8 ± 0.8	2.66 ± 0.06	20.0 ± 0.4	61.5 ± 1.3	30 ± 1

Uncertainties in the ^{10}Be, ^{26}Al, and ^{36}Cl concentrations are typically 2–3%, while those for ^{41}Ca concentrations are typically 5–10% (and >10% for ^{41}Ca concentrations <1 dpm/kg). To verify pairing and constrain the preatmospheric size, we also measured ^{10}Be and ^{26}Al in the stone fraction of FRO 93009 and 01172, following procedures described elsewhere (Welten et al. 2001). The results of these two samples are listed in Table 4.

Terrestrial Ages

To determine the terrestrial ages, we used four different methods, depending on the age, shielding conditions and exposure history. For eight meteorites with high concentrations of ^{36}Cl (>20 dpm/kg) and ^{41}Ca (>18 dpm/kg), we determined the terrestrial age based on the ^{14}C concentration, assuming average saturation values of 46 ± 7 dpm/kg for H chondrites and 51 ± 8 dpm/kg for L chondrites (Jull et al. 1993). We did not use the ^{14}C/^{10}Be method, because we only have ^{10}Be data of the metal fraction, whereas this method requires ^{10}Be in the bulk (or stone fraction). For three of these meteorites, the absence of ^{14}C only gives a lower age limit of 34–40 kyr, whereas the other five meteorites show ^{14}C ages ranging from 6 ± 1 kyr (FRO 99031) to 32 ± 4 kyr (FRO 90072).

In the past, terrestrial ages of Antarctic meteorites were mostly determined from the ^{36}Cl concentration in the metal phase, assuming a constant production rate of 22.1 ± 2.8 dpm/kg (Nishiizumi et al. 1989; Nishiizumi 1995). More recently, it was shown that the production rate of ^{36}Cl in the metal phase of large chondrites is more variable, ranging from 14–21 dpm/kg in the FRO 90174 shower (Welten et al. 1999), 6–20 dpm/kg in the QUE 90201 shower (Welten et al. 2005) and 0.5–12 dpm/kg in the Gold Basin shower (Welten et al. 2003). We thus calculated the terrestrial ages using shielding-corrected methods based on the ^{36}Cl/^{10}Be and ^{41}Ca/^{36}Cl ratios (Lavielle et al. 1999; Nishiizumi and Caffee 1998). Details of these shielding-corrected methods are discussed in Appendix 1. Finally, for three meteorites for which ^{41}Ca was measured (but not ^{36}Cl), we determined the terrestrial age from the ^{41}Ca concentration only. Since the ^{10}Be concentrations of 5–6 dpm/kg indicate that these meteorites were small objects in space, we assumed an average saturation value of 24 ± 4 dpm/kg (2σ).

Noble Gas Measurements

Samples consisting of one or several chips totalling 100–150 mg were wrapped in aluminum foil and preheated for about 24 h at 130 °C to desorb loosely bound atmospheric noble gases. Helium, neon, and argon were released, separated, and analyzed as described previously (Wieler et al. 1989). The measured noble gas concentrations, as listed in Table 3, are accurate to ~5%; isotopic ratios of Ne and Ar are accurate to 0.5–1.0%. We note that the concentrations of cosmogenic ^{3}He, ^{21}Ne, and ^{38}Ar as well as radiogenic ^{4}He and ^{40}Ar in FRO 93002 and 93054 are in the same range as those of the FRO 90001 H-chondrite group (Welten et al. 1999), suggesting they probably belong to the same group. The deconvolution of measured noble gas concentrations in trapped, radiogenic, and cosmogenic components are discussed in Appendix 2, while the methods for calculating cosmic-ray exposure (CRE) ages are discussed in Appendix 3.

TERRESTRIAL AGES AND PAIRING

H Chondrites

Thirteen of the fourteen H chondrites measured in this study show low concentrations of cosmogenic ^{10}Be in the metal phase, in a relatively narrow range from 2.6 to 3.7 dpm/kg, indicating high shielding conditions. On the other hand, the shorter-lived radionuclides each show two clusters of 10 and 3 members: ^{26}Al clusters at 1.9–2.6 and 2.8–3.1 dpm/kg, ^{36}Cl at 12–16 and 20–22 dpm/kg and ^{41}Ca at 8–10 and 18–21 dpm/kg (Table 3). The concentrations of these two clusters are very similar to those of two previously identified H5/6 chondrite pairing groups: FRO 90001 and FRO 90174 (Welten et al. 1999, 2001).

FRO 90174 Shower

Figure 2 shows that the ^{36}Cl/^{10}Be and ^{41}Ca/^{36}Cl ratios in ten H chondrites overlap with those of the FRO 90174 shower and are consistent with an average terrestrial age of ~100 kyr. The overlapping ^{36}Cl/^{10}Be and ^{41}Ca/^{36}Cl ratios, low ^{10}Be concentrations and similar terrestrial ages provide strong evidence that these ten H chondrites are part of the same shower. The new members of this shower show much less

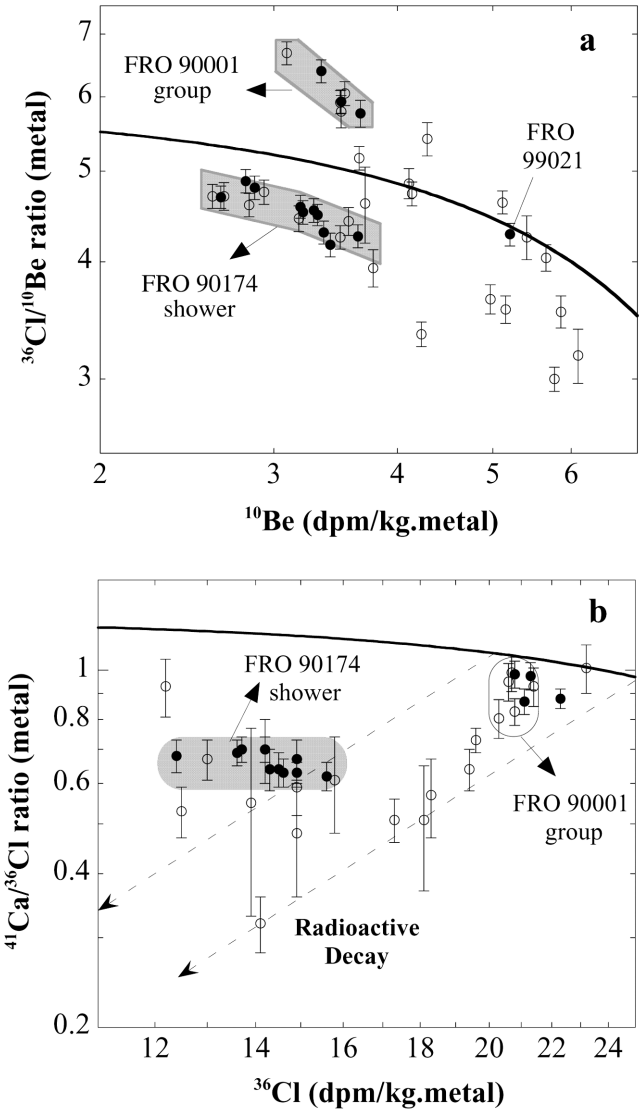

Fig. 2. a) The concentration of ^{10}Be versus ^{36}Cl/^{10}Be ratio and b) the concentration of ^{36}Cl versus ^{41}Ca/^{36}Cl ratio in FRO H chondrites. The results show that ten of the new H chondrites belong to the FRO 90174 shower, whereas three belong to the FRO 90001 pairing group. Closed symbols represent results from this work; open symbols data are from Welten et al. (1999; 2001).

variation in the measured ^{41}Ca/^{36}Cl ratios (0.62–0.70) than those measured previously (0.48–0.93). This is due to the smaller uncertainties in the measured ^{41}Ca/Ca ratios, which are now 5–10% compared to 10–25% previously (Welten et al. 2001). Ironically, many of the new members of the FRO 90174 shower are of petrologic type 3 or 4 and were selected to avoid pairing with the two H5/6 chondrite showers. The cosmogenic nuclide results thus corroborate that the specimens of the FRO 90174 shower are small fragments (the largest one, FRO 01049, is merely 44.1 g) of a heterogeneous lithology which should be classified as an H3–6 chondrite breccia. This conclusion is consistent with petrographic

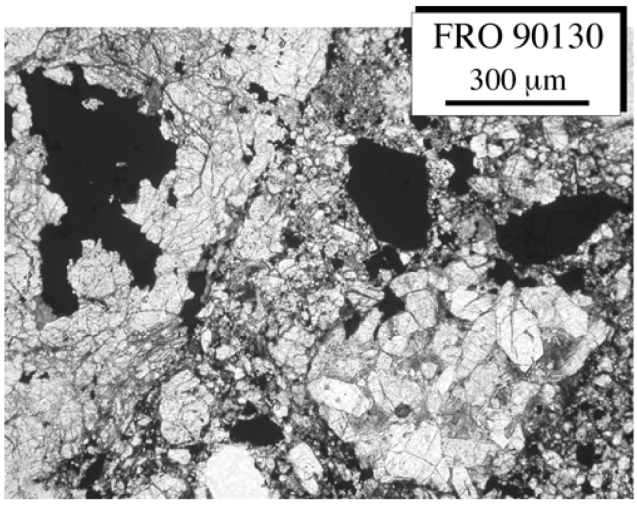

Fig. 3. An optical micrograph of the FRO 90130 breccia, showing petrographic type 3 (the porphyritic lithic fragment on the lower right) and type 6 clasts (the relatively coarse, granoblastic lithic fragments on the upper left).

observations of a thin section of FRO 90130, a heterogeneous H-chondrite breccia which shows mm to cm sized clasts ranging from petrographic type 3 to 6 (Fig. 3). The identification of a heterogeneous H-chondrite shower at FRO confirms the hypothesis (Welzenbach et al. 2005) that many brecciated ordinary chondrite showers may have gone unnoticed in the Antarctic meteorite collections.

FRO 90001 Pairing Group

The high ^{36}Cl/^{10}Be and ^{26}Al/^{10}Be ratios in three of the four remaining H chondrites, FRO 93002, 93054, and 95012, overlap with those of the FRO 90001 H5/6 pairing group. The pairing is confirmed by the cosmogenic and radiogenic noble gas concentrations in FRO 93002/93054 (Table 5), which overlap with those of the FRO 90001 group (Welten et al. 1999). These fragments are all pretty weathered in hand-specimen, corresponding to ANSMET weathering category B (moderate rustiness). Unlike the members of the FRO 90174 shower, which are for >90% covered with fusion crust, all seven members of the FRO 90001 pairing group are nearly devoid of fusion crust and look like the result of fragmentation on the ice rather than the result of atmospheric fragmentation. This interpretation is consistent with the constant ^{36}Cl concentration of 20.9 ± 0.4 dpm/kg, which indicates minor differences in shielding. After correction for radioactive decay of ^{36}Cl during the terrestrial residence time of ~40 kyr, we obtain an average ^{36}Cl concentration of 22.9 ± 0.5 dpm/kg at the time of fall, indicating a small preatmospheric size (R = 10–30 cm). We therefore refer to FRO 90001 as a pairing group rather than a meteorite shower.

FRO 99021 is the only H chondrite studied in this work that is not part of these two pairing groups (Fig. 2). The ^{41}Ca/^{36}Cl ratio of 0.88 ± 0.04 yields a terrestrial age of 30 ± 20 kyr,

Table 5. Concentrations of noble gases (in 10^{-8} cm^3 STP/g) in four FRO chondrites and cosmic-ray exposure ages (in Myr) derived from cosmogenic ^{3}He (T3), ^{21}Ne (T21), and ^{38}Ar (T38). Production rates of ^{3}He and ^{21}Ne were calculated according to Eugster (1988), those of ^{38}Ar according to Schultz et al. (1991). The low ^{3}He ages of FRO 93002/93054 (in italics) were not included in the average age, since they are due to loss of He. The minimum ^{21}Ne ages, T(min), are based on maximum production rates of 0.350 for H chondrites and 0.375 × 10^{-8} cm^3 STP g^{-1} Myr^{-1} for L chondrites. The last column shows the adopted ages, T(CRE). For 93002/93054 these are based on the ^{10}Be/^{21}Ne and ^{26}Al/^{21}Ne ages of other members of the FRO 90001 pairing group (Welten et al. 2001), whereas for FRO 93009, the adopted age is the average of the ^{10}Be/^{21}Ne and ^{26}Al/^{21}Ne ages determined in this work.

FRO	^{3}He	^{4}He	^{20}Ne	^{21}Ne	^{22}Ne	^{22}Ne/^{21}Ne	^{36}Ar	^{38}Ar	^{40}Ar	^{38}Arc	T3	T21	T38	T (avg)	T (min)	T (CRE)
93002	3.09	263	1.58	1.74	1.85	1.064	0.56	0.27	2939	0.19	*1.9*	4.5	4.7	4.6 ± 0.5	5.0	8 ± 1
93054	3.66	449	1.54	1.72	1.83	1.060	0.55	0.26	3382	0.17	*2.2*	4.3	4.4	4.3 ± 0.4	4.9	8 ± 1
93005	17.0	395	3.63	3.61	4.02	1.106	0.62	0.43	874	0.36	10.6	10.7	9.0	10 ± 1	9.6	10 ± 1
93009	18.1	267	4.86	5.27	5.67	1.072	3.94	1.08	451	0.45	11.1	13.1	10.6	12 ± 1	14.0	16 ± 2

whereas the absence of ^{14}C indicates an age >40 kyr. We thus adopt an age of 45 ± 5 kyr. Finally, the two H chondrites from nearby ice fields, JOH 01001 and WAL 01001, show relatively young terrestrial ages of 10 ± 20 and 30 ± 20 kyr, respectively.

H/L-Chondrite Ratio

Interestingly, of the 40 more or less randomly selected H chondrites, 19 are part of the FRO 90174 shower, and 7 are part of the FRO 90001 pairing group. It was previously suggested that the high H/L chondrite ratio of ~3 was due to one or two large H chondrite showers (Delisle et al. 1989, 1993; Welten et al. 1999). If the present sample of 40 H-chondrite specimens is representative of the whole FRO collection, then about 2/3 of all H-chondrites are part of these two pairing groups. The FRO collections of 1984–2001 contain a total of 622 classified meteorites. Of those, 467 are H and 123 are L (or L/LL) chondrites, which corresponds to an H/L-chondrite ratio of 3.8. Although there may be other small H-chondrite showers in the FRO collection, it seems plausible that the high H/L ratio is mainly due to the large FRO 90174 shower, since it had an estimated preatmospheric mass of 7.5–15 metric tons, includes specimens of all petrologic types (3–6), and was scattered over a large part (~7 × 1 km^2) of the FRO stranding area (Fig. 1a). The FRO 90001 pairing group, on the other hand, represents a small object, includes only H5/6 chondrites, and is mainly concentrated on the firn-ice edge (Fig. 1a).

The presence of two pairing groups in the FRO H-chondrite collection is also supported by the mass distribution of Fig. 4a, which is not smooth like the L-chondrite distribution, but shows two humps. The first hump, at ~100 g, is due to the FRO 90001 pairing group, which probably contains several tens of fragments in the 10–100 g range. The second and largest hump at ~30 g is due to the FRO 90174 shower, which is dominated by many small fragments of <30 g. This is even more clear in Fig. 4b, which shows that the H chondrites show an excess of >300 specimens <30 g relative to the FRO L chondrites and the estimated mass distribution of infalling meteorites (Halliday et al. 1989). We thus conclude that the FRO 90174 shower probably contains more than 300 small fragments.

L Chondrites

Seven out of nine FRO L chondrites show relatively high concentrations of ^{36}Cl (21–27 dpm/kg) and ^{41}Ca (18–25 dpm/kg), indicating terrestrial ages of less than 50 kyr. Differences in the ^{36}Cl/^{10}Be versus ^{10}Be systematics combined with ^{14}C terrestrial ages in FRO L chondrites (Fig. 5) suggest that they represent at least six different falls.

FRO 90052/90172

One cluster in Fig. 5 is formed by FRO 90052 (L4) and 90172 (L5), two small L chondrites that were found within ~100 m of each other on the firn-ice edge. They show almost identical cosmogenic radionuclide concentrations and elevated ^{36}Cl/^{10}Be ratios, which plot ~25% above the ^{36}Cl/^{10}Be versus ^{10}Be curve for falls. These high ^{36}Cl/^{10}Be ratios are partly due to the high ^{36}Cl concentrations of 26–27 dpm/kg, which are somewhat above the normal range of 19–25 dpm/kg (Nishiizumi 1995). In addition, the high ^{26}Al/^{10}Be ratios of 0.82–0.84 suggest that these two L chondrites either had a short CRE age of ~4 Myr, which results in undersaturation of ^{10}Be by ~15%, or a complex CRE history with a short second-stage exposure. Although noble gas measurements are needed to distinguish between a short or a complex CRE history, we conclude that these two L chondrites are paired. Interestingly, FRO 90052 and 90172 also show distinct metal compositions (Table 1), i.e., the concentrations of Ni (20–22 wt%) and Co (0.92–0.95 wt%) are higher than for most other L chondrites (10–18 wt% Ni). The ^{14}C concentration of 3.2 ± 0.7 dpm/kg in FRO 90052 yields a terrestrial age of 23 ± 2 kyr.

FRO 93005/99016/99028

Based on the similar concentrations of ^{10}Be, ^{26}Al, and

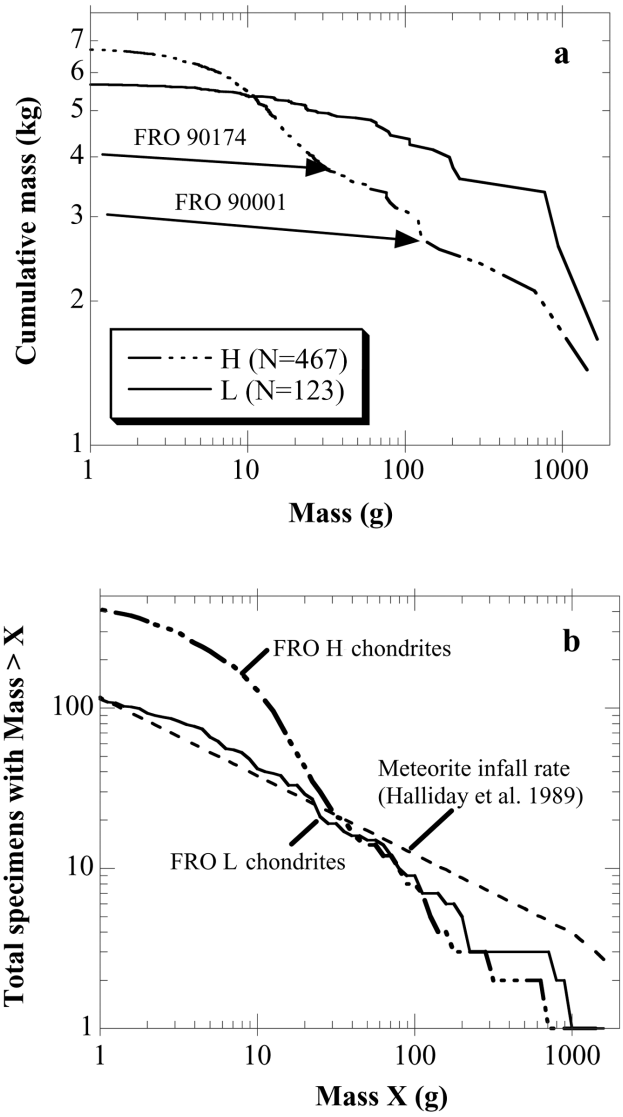

Fig. 4. a) The cumulative mass distribution of Frontier Mountain H and L chondrites with masses ranging from 1–2000 g. The L-chondrite distribution is relatively smooth for masses <200 g, whereas the H-chondrite mass distribution shows two humps, at ~100 g and ~30 g, which are presumably related to the two pairing groups, FRO 90001 and FRO 90174, respectively. b) The cumulative numerical distribution of Frontier Mountain H and L chondrites with masses ranging from 1 to 2000 g. The H-chondrite distribution shows a large excess (~300%) of masses <30 g relative to the estimated mass distribution of infalling meteorites (Halliday et al. 1989), normalized to a total mass of ~6 kg for all masses <2 kg. This large excess suggests that most of the small H chondrites are part of the large FRO 90174 shower. The L-chondrite distribution shows only a very small excess (~10%) of meteorites <30 g, indicating that pairing is less prominent among FRO L chondrites.

^{36}Cl in FRO 93005, 99016, and 99028, it is possible that these three L chondrites represent a second pairing group (Fig. 5). However, the ^{41}Ca concentration in FRO 99016 is 12–20% lower than in FRO 93005/99028, suggesting that the meteorite found in Meteorite Valley is 20–30 kyr older than

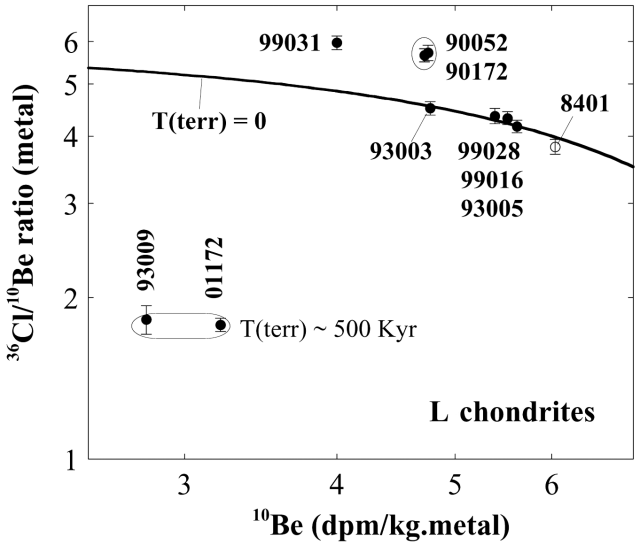

Fig. 5. a) The concentration of ^{10}Be versus the ^{36}Cl/^{10}Be ratio in FRO L chondrites.

the two L chondrites found on the scatter field. This is confirmed by the concentrations of cosmogenic ^{14}C, which yields a terrestrial age of >40 kyr ago for FRO 99016, compared to ages of 27 ± 2 and 21 ± 3 kyr for 93005 and 99028, respectively. Although we cannot exclude that the two large L chondrites from the scatter field are paired, we assume for now that they are distinct falls, mainly based on a factor of 2 difference in cosmogenic ^{14}C. The CRE age of 10 ± 1 Myr for FRO 93005 excludes pairing with FRO 8401, for which previously an age of ~25 Myr was reported (Welten et al. 1999).

FRO 93009/01172

Two L chondrites, FRO 93009 (L4) and 01172 (L3), show very low concentrations of ^{36}Cl (5.6–5.8 dpm/kg) and ^{41}Ca (0.5–0.6 dpm/kg), suggesting terrestrial ages of ~500 kyr (Table 3). Since these ages are an order of magnitude higher than those of other FRO L chondrites, it is likely that these two meteorites are paired, even though they were found more than 3 km apart, on opposite sides of Frontier Mountain (Fig. 1). Interestingly, the low concentrations of ^{10}Be and ^{26}Al in the metal phase of FRO 93009/01172 are only partly due to the high terrestrial age, and also seem to indicate higher-than-average shielding conditions. We thus measured ^{10}Be and ^{26}Al in the stone fraction of these two L chondrites to constrain their preatmospheric size (Table 4). To compare the results with model calculations for L-chondrite falls, we increased the measured ^{10}Be and ^{26}Al concentrations in the stone fraction by 4–6% to account for dilution of silicates with oxidized metal, and corrected for radioactive decay of ^{10}Be and ^{26}Al (during the terrestrial residence time of ~500 kyr). Figure 6 shows the ^{10}Be concentrations in the stone and metal phase of FRO 93009 and 01172 at the time of fall, compared to calculated production rates. The results

indicate that FRO 93009 and 01172 were part of an object with a preatmospheric radius of ~80 cm, similar to the FRO 90174 H-chondrite shower. This implies that these two small L chondrites are the (only two?) survivors of an old meteorite shower, that fell near the FRO stranding area ~0.5 Myr ago. Based on its large preatmospheric size this shower may have contained many tens or hundreds of fragments.

Including previous cosmogenic nuclide results for FRO 8401 (Welten et al. 2001), the ten FRO L chondrites represent seven or eight different falls, of which one has a very old terrestrial age of 500 ± 25 kyr, while the others have terrestrial ages ranging from 6 kyr to ~45 kyr. The L chondrite found at Miller Butte is also relatively young with a terrestrial age of 30 ± 20 kyr.

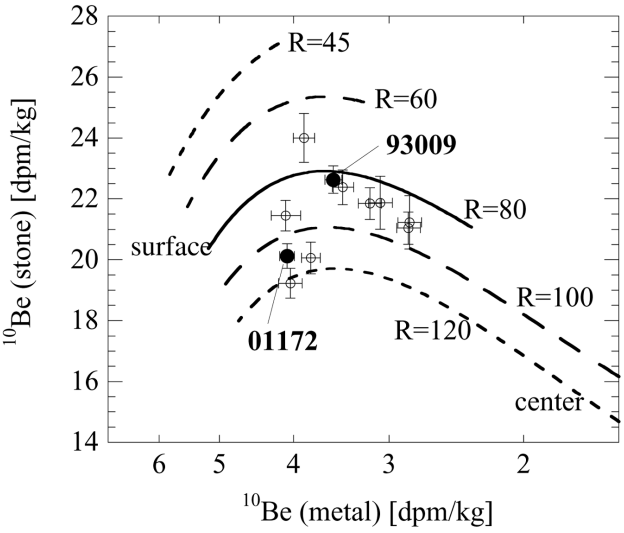

Fig. 6. Concentration of ^{10}Be at the time of fall in the metal and stone fraction of the FRO 93009 and 01172 L chondrites. The results are compared with those of the FRO 90174 H chondrite shower (open symbols) and with calculated production rates for chondritic objects with radii ranging from 45–120 cm.

Meteorite Concentration Mechanism at FRO

The new terrestrial age and pairing results, combined with those previously obtained by Welten et al. (1999 and 2001), add quantitative information to the proposed meteorite trapping mechanism at FRO (Delisle et al. 1989; Delisle 1993; Folco et al. 2002). In particular, the geographic distribution of the FRO 90001 and 90174 showers and that of the FRO 93009/01172 pair (Fig. 1) allow us to address important issues regarding the role of the wind-drift in redistributing meteorite specimens on the ice surface and the stability of the meteorite trap over the last glacial maximum.

The distribution of the FRO 90001 pairing group is shown in Fig. 1a. With recovered masses of 665 and 1438 g, FRO 93002 and 93054 are the largest fragments of this meteorite, and were found in the scatter field. FRO 90001, 90050, 90073, and 90152 are small fragments (<76.1 g) found at the firn-ice edge. The 44 g FRO 95012 fragment was found in between the two above find sites. This distribution agrees with the previous hypothesis by Delisle et al. (1993), which predicts that the firn-ice edge is an aeolian accumulation and provides firm evidence confirming the wind-drift model subsequently proposed by Folco et al. (2002). The latter model, based on local morphology, wind direction and wind-drift experiments (namely, wind-driven rock races), envisages that meteorites lighter than ~200 g are wind-blown across the scatter field in a northeastward direction by katabatic winds and accumulate at the firn-ice edge.

The FRO 93009 and 01172 paired fragments, which fell ~500 kyr ago, were found in two moraines about 3 km apart, i.e., the Meteorite Valley and the Central Moraines, respectively. These moraines are currently nourished by the two different ice flows passing opposite ends of the mountain (Fig. 1a). Although we do not know if the local glaciological conditions 500 kyr ago were exactly the same as those today, it seems plausible that the two meteorites ended up in their present locations under glaciological conditions which were very similar to those acting today. According to the general meteorite concentration model (e.g., Whillans and Cassidy 1983), the two meteorites fell (as part of a larger shower) some distance apart in the snow accumulation zone, upstream from FRO, were incorporated in the two ice flows passing opposite sides of FRO and were released in the blue ice area northeast of FRO. Since the cosmogenic nuclide data of FRO 93009 and 01172 clearly indicate a large preatmospheric size (R ~ 0.8 m), it is likely that many more (tens or hundreds) fragments of this large meteorite were released in the FRO blue ice area. Apparently, due to the combined action of wind-transport and ice flow draining into the Rennick Glacier, most of these fragments were flushed out of the FRO area during the past ~500 kyr. In fact, the relatively small size of FRO 93009 and 01172 (65 and 150 g, respectively) suggests that they must have been released relatively close to their present location of find, otherwise they would have been blown northeastward and flushed out of the stranding area as well. Based on the terrestrial age of 500 ± 25 kyr for the FRO 93009/01172 pair, we infer that the Meteorite Valley and Central Moraines are sites of the ice field where old plateau ice has continuously or intermittently been exhumed during the past 400–500 kyr.

The FRO 90174 shower has a terrestrial age of 100 ± 20 kyr. Of the fifteen specimens of this shower found in the Meteorite Valley, three were found in a supraglacial morainic deposit on an ice slope at the foot of the northern flank of the valley (Fig. 1b). This deposit extends for ~100 × 40 m in an overall southwest-northeast direction. The deposit is a mixture of large angular boulders likely fallen from the valley wall and much smaller-sized and reworked glacial drift similar to that found in the Meteorite Valley (the central deposit with triangular outline in Fig. 1b, described in detail

by Folco et al. 2002). Its upper limit runs at an elevation of ~2100 m and lies ~30 to ~40 m above the Meteorite Valley, (i.e., ~30 to ~40 m above the present-day ice level at the mouth of the valley), indicating a former high stand of the ice (Fig. 1b). A stretch of snow cover does not allow spatial and temporal relationships to be established between this deposit and the Meteorite Valley; nevertheless, the presence of FRO 90174 (paired) fragments in both locations (Fig. 1a) indicates that the moraine deposits are one single body recording an ice reduction of several tens of meters in the Meteorite Valley since the fall of the FRO 90174 shower during the last glacial cycle. This reduction in ice thickness is on the low end of the range of 30–150 m predicted by the ice-flow model of Delisle (1993) for blue ice areas at altitudes of ~2200 m. Our evidence of moderate ice level changes supports the stability of the FRO meteorite trap over the last glacial cycle (Folco et al. 2002), whereas the complex exposure history of a bedrock sample collected from <100 m above the present ice level indicates ice-level variations >100 m on a longer (a few Myr) time scale (Welten et al. 1999). Additional cosmogenic nuclide studies on FRO bedrock samples collected from higher altitudes (up to 2795 m) are in progress to constrain the last overriding of the Frontier Mountain Range, which presumably occurred during the Tertiary (Delisle et al. 1989).

All eight meteorites found on the main blue ice field (scatter field) are younger than ~50 kyr (Fig. 7). Although these meteorites may be a mixture of direct infall and specimens released from the ablating ice, the absence of meteorites older than 50 kyr on the scatter field suggests that the blue ice itself is younger than 50 kyr. The possible relationship between terrestrial age of these meteorites and the stratigraphy of the ice on which they were found will be discussed elsewhere (Folco et al. 2006). The observation that some of the meteorites in the eastern part of the firn-ice edge are up to ~150 kyr old (Welten et al. 2001) suggests that meteorites, which were exhumed from the blue ice in the scatter field and blown into the firn-ice edge, were stored in this trap for up to ~100 kyr. These long storage times in the firn-ice edge are higher than the maximum calculated storage time of ~50 kyr based on the present eastward ice flow rate of ~9 cm/yr measured at one location in the firn-ice edge, which extends for 4–5 km (Folco et al. 2002). The higher storage times inferred from terrestrial ages could indicate that the eastward ice flow rate along the firn-ice edge either is not uniform (and is on the average much lower, say ~5 cm/yr) and/or was a factor of 2–3 lower in the last glacial stage (e.g., Coren et al. 2003) when most of this storage took place. An alternative explanation is that the meteorites which were released from the blue ice during the last glacial stage—when horizontal ice flow rates were presumably a factor of 2–3 lower (Delisle 1993; Coren et al. 2003)—were significantly older than 50 kyr, thus requiring shorter storage times in the firn-ice edge, more consistent with those calculated under the present conditions. No matter which scenario is closer to reality, the local glaciological conditions in the scatter field and firn-ice edge must have been relatively stable during the last glacial cycle to preserve meteorites for up to ~150 kyr in a stranding site whose efficiency to trap meteorites seems so sensitive to small changes in ice flow direction or rate.

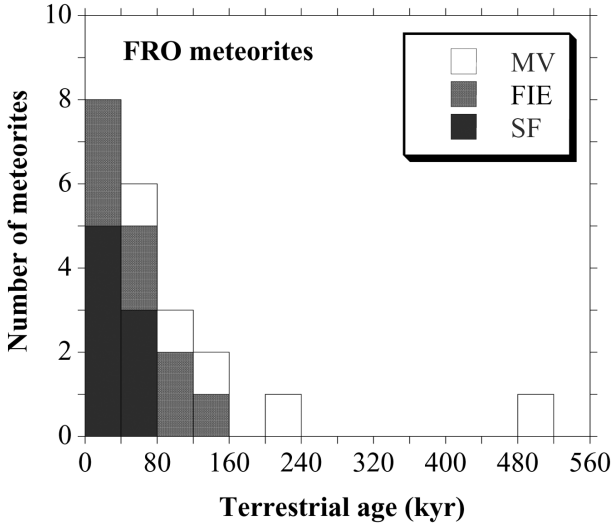

Fig. 7. Histogram of terrestrial ages of 21 FRO meteorites from the Meteorite Valley (MV), the scatter field (SF), and the firn-ice edge (FIE). Meteorites found on different parts of the stranding area show a clear trend in terrestrial age, decreasing from MV > FIE > SF.

CONCLUSIONS

The measured concentrations of cosmogenic radionuclides in the metal fraction of 14 H chondrites from the FRO collection show that 13 out of the 14 selected samples are part of the two large pairing groups, FRO 90001 and 90174, that were identified previously. Both of these groups belong to the prominent peak at ~7 Myr in the exposure age histograms of H-chondrites (Welten et al. 2001). The largest pairing group, FRO 90174, now encompasses nineteen members spread out over a large part of the stranding area. Since this pairing group includes samples of petrologic type 3–6, this shower must be classified as an H3-6 chondrite breccia. The large preatmospheric size (R = 80–100 cm), wide geographic distribution and heterogeneous nature of the FRO 90174 pairing group suggest that more than 50% of all H chondrites found at FRO belong to this shower. In addition, the mass distribution of FRO H-chondrites shows a three- to four-fold excess of specimens <30 g relative to those of FRO L chondrites as well as estimated meteorite infall rates of Halliday et al. (1989). The combined evidence of cosmogenic nuclides, petrologic studies and mass distributions suggests that >300 of all 467 H chondrites found at the FRO "meteorite trap" are part of the FRO 90174 shower, which thus largely explains the high H/L-chondrite ratio of ~3.8 at FRO. Some of the fragments of the FRO 90174 shower were found in a supraglacial morainic deposit on an ice slope 30–40 m above the present-day ice level at the mouth of the valley. These

meteorites must have been deposited by a former high stand of the ice during the last glacial maximum (or a former glaciation). The find locations of these meteorites thus argue against large fluctuations of the ice at FRO in the recent past, supporting the stability of the meteorite trap over the last glacial cycle.

The FRO 90001 pairing group includes seven members, which were all found within ~2 km of the largest member (FRO 93054) and are nearly devoid of fusion crust. Combined with the small preatmospheric size (R < 30 cm), these observations suggest that this object broke up on the ice, after which the smaller fragments were redistributed by wind-controlled transport. We estimate that this pairing group includes several tens of specimens.

The cosmogenic nuclide concentrations for nine new FRO L chondrites suggest seven independent falls. Six out of these seven falls are younger than 50 kyr. Three of these L chondrites were found on the main blue ice field and confirm the trend that all meteorites found on the scatter field are younger than 50 kyr. The absence of meteorites older than 50 kyr suggests that the bulk of the ablating ice at FRO is younger than 50 kyr. Finally, two L chondrites, FRO 93009 and 01172 have a very long terrestrial age of ~500 kyr. These paired fragments are much older than any of the other FRO meteorites, which are all younger than 250 kyr. The concentrations of cosmogenic ^{10}Be in the stone and metal fraction indicate that these two meteorites are small fragments of a large pre-atmospheric object, similar in size (R ~80 cm) to the FRO 90174 H-chondrite shower. The find locations of these two paired L-chondrite fragments on opposite sides of Frontier Mountain suggest that the two ice flows passing both ends of the mountain are from the same source area on the plateau. We also conclude that the Meteorite Valley and Central moraines are sites of the FRO ice field where plateau ice has been exhumed and meteorites have been stored for the past 400–500 kyr.

Acknowledgments–We thank the Italian Programma Nazionale delle Ricerche in Antartide (PNRA) for providing us with the meteorite samples. This work was supported, in part, by PNRA (LF), NASA grant NAG5-12846, and NSF grant OPP 0230419 (KCW and KN), and a LLNL-CAMS grant. We thank R. Finkel for assistance with AMS measurements, which were performed under the auspices of the U.S. DOE by LLNL under contract W-7405-ENG-48. We thank K. Marti and G. Delisle for constructive reviews and U. Krähenbühl for editorial handling.

Editorial Handling—Dr. Urs Krähenbühl

REFERENCES

Alexeev V. A. 1998. Parent bodies of L and H chondrites: Times of catastrophic events. *Meteoritics & Planetary Science* 33:145–152.

Coren F., Delisle G., and Sterzai P. 2003. Ice dynamics of the Allan Hills meteorite concentration sites revealed by satellite aperture radar interferometry. *Meteoritics & Planetary Science* 38:1319–1330.

Davis J. C., Proctor I. D., Southon J. R., Caffee M. W., Heikkinen D. W., Roberts M. L., Moore T. L., Turteltaub K. W., Nelson D. E., Loyd D. H., and Vogel J. S. 1990. LLNL/UC AMS facility and research program. *Nuclear Instruments and Methods B* 52: 269–272.

Delisle G. 1993. Global change, Antarctic meteorite traps and the East Antarctic ice sheet. *Journal of Glaciology* 39:397–408.

Delisle G. et al. 1989. Meteorite finds near the Frontier Mountain Range in northern Victoria Land. *Geologische Jahrbuch* E38: 483–513.

Delisle G., Franchi I., Rossi A., and Wieler R. 1993. Meteorite finds by EUROMET near Frontier Mountains, North Victoria Land, Antarctica. *Meteoritics* 28:126–129.

Donahue D. J., Linick T. W., and Jull A. J. T. 1990. Isotope-ratio and background corrections for accelerator mass spectrometry radiocarbon measurements. *Radiocarbon* 32:135–142.

Eugster O. 1988. Cosmic-ray production rates of ^{3}He, ^{21}Ne, ^{38}Ar, ^{83}Kr and ^{126}Xe in chondrites based on ^{81}Kr-Kr exposure ages. *Geochimica et Cosmochimica Acta* 52:1649–1662.

Ferraris C., Folco L., Mellini M., and Zeoli A 2003. Meteorites: 174 new finds from Frontier Mountain and other blue ice fields in the Rennick and David Glaciers regions (Antarctica, 2001–2002). *Terra Antartica Reports* 8:185–192.

Folco L. and Bland P. 1994. Meteorites from the 1990/91 EUROMET Expedition to Frontier Mountain, northern Victoria Land, Antarctica. *Terra Antarctica* 1:138–142.

Folco L., Capra A., Chiappini M., Frezzotti M., Mellini M., and Tabacco I. E. 2002. The Frontier Mountain meteorite trap (Antarctica). *Meteoritics & Planetary Science* 37:209–228.

Folco L., Welten K. C., Nishiizumi K., and Hillegonds D. J. 2004. Discovery and terrestrial age of FRO 01149, and extremely small, weathered and old H chondrite found on top of Frontier Mountain, Antarctica (abstract). *Meteoritics & Planetary Science* 39:A40.

Folco L., Welten K. C., Jull A. J. T., Nishizumi K., and Zeoli A. Forthcoming. Meteorites constrain the age of Antarctic ice at the Frontier Mountain blue ice field (northern Victoria Land). *Earth and Planetary Science Letters*.

Graf T. and Marti K. 1995. Collisional history of H chondrites. *Journal of Geophysical Research* E100:21,247–21,263.

Graf Th., Baur H., and Signer P. 1990. A model for the production of cosmogenic nuclides in chondrites. *Geochimica et Cosmochimica Acta* 54:2521–2534.

Halliday I., Blackwell A. T., and Griffin A. A. 1989. The flux of meteorites to Earth's surface. *Meteoritics* 24:173–178.

Jull A. J. T., Donahue D. J., Cielaszyk E., and Wlotzka F. 1993. ^{14}C terrestrial ages and weathering of 27 meteorites from the southern High Plains and adjacent areas (USA). *Meteoritics* 28: 188–195.

Lavielle B., Marti K., Jeannot J.-P., Nishiizumi K., and Caffee M. W. 1999. The ^{36}Cl-^{36}Ar-^{40}K-^{41}K records and cosmic-ray production in iron meteorites. *Earth and Planetary Science Letters* 170:93–104.

Leya I., Lange H.-J., Neumann S., Wieler R., and Michel R. 2000. The production of cosmogenic nuclides in stony meteoroids by galactic cosmic-ray particles. *Meteoritics & Planetary Science* 35:259–286.

Leya I., Graf Th., Nishiizumi K., and Wieler R. 2001. Cosmic-ray production rates of helium, neon, and argon isotopes in H chondrites based on chlorine-36/argon-36 ages. *Meteoritics & Planetary Science* 36:963–973.

Makjanic J., Vis R. D., Hovenier J. W., and Heymann D. 1993. Carbon in the matrices of ordinary chondrites. *Meteoritics* 28: 63–70.

Marti K. and Graf T. 1992. Cosmic-ray exposure history of ordinary chondrites. *Annual Review of Earth and Planetary Science* 20: 221–243.

Nishiizumi K. 2004. Preparation of ^{26}Al AMS standards. *Nuclear Instruments and Methods B* 223–224:388–392.

Nishiizumi K. and Caffee M. W. 1998. Measurements of cosmogenic calcium-41 and calcium-41/chlorine-36 terrestrial ages (abstract). *Meteoritics & Planetary Science* 33:A117.

Nishiizumi K., Elmore D., Ma X. Z., and Arnold J. R. 1984. ^{10}Be and ^{26}Al depth profiles in an Apollo 15 drill core. *Earth and Planetary Science Letters* 70:157–163.

Nishiizumi K., Elmore D., and Kubik P. W. 1989. Update on terrestrial ages of Antarctic meteorites. *Earth and Planetary Science Letters* 93:299–313.

Nishiizumi K., Caffee M. W., Jeannot J.-P., Lavielle B., and Honda M. 1997. A systematic study of the cosmic-ray exposure history of iron meteorites: beryllium-10-chlorine-36/beryllium-10 terrestrial ages (abstract). *Meteoritics & Planetary Science* 32: A100.

Nishiizumi K., Caffee M. W., and DePaolo D. J. 2000. Preparation of ^{41}Ca AMS standards. *Nuclear Instruments and Methods B* 172: 399–403.

Scherer P., Schultz L., and Loeken T. 1994. Weathering and atmospheric noble gases in chondrites. In *Noble gas geochemistry and cosmochemistry,* edited by Matsuda J. Tokyo: Terra Scientific Publishing Company. pp. 43–53.

Schultz L., Weber H. W., and Begemann F. 1991. Noble gases in H chondrites and potential differences between Antarctic and non-Antarctic meteorites. *Geochimica et Cosmochimica Acta* 55:59–66.

Stöffler D., Keil K., and Scott E. R. D. 1991. Shock metamorphism of ordinary chondrites. *Geochimica et Cosmochimica Acta* 54: 3845–3867.

Welten K. C., Nishiizumi K., Caffee M. W., Schäfer J., and Wieler R. 1999. Terrestrial ages and exposure ages of Antarctic H chondrites from Frontier Mountain, North Victoria Land. *Antarctic Meteorite Research* 12:94–107.

Welten K. C., Nishiizumi K., Masarik J., Caffee M. W., Jull A. J. T., Klandrud S. E., and Wieler R. 2001. Cosmic-ray exposure history of two Frontier Mountain H-chondrite showers from spallation and neutron-capture products. *Meteoritics & Planetary Science* 36:301–317.

Welten K. C., Caffee M. W., Leya I., Masarik J., Nishiizumi K., and Wieler R. 2003. Noble gases and cosmogenic radionuclides in the Gold Basin L4-chondrite shower: Thermal history, exposure history and pre-atmospheric size. *Meteoritics & Planetary Science* 38:157–173.

Welten K. C., Nishiizumi K., Finkel R. C., Hillegonds D. J., Jull A. J. T., Franke L., and Schultz L. 2004. Exposure history and terrestrial ages of ordinary chondrites from the Dar al Gani region, Libya. *Meteoritics & Planetary Science* 39:481–498.

Welzenbach L. C., McCoy T. J., Grimberg A., and Wieler R. 2005. Petrology and noble gases of the regolith breccia MAC 87302 and implications for the classification of Antarctic meteorites (abstract #1425). 35th Lunar and Planetary Science Conference. CD-ROM.

Wieler R., Graf T., Pedroni A., Signer P., Pellas P., Fieni C., Suter M., Vogt S., Clayton R. N., and Laul J. C. 1989. Exposure history of the regolithic chondrite Fayetteville: II. Solar-gas-free light inclusions. *Geochimica et Cosmochimica Acta* 53:1449–1459.

Whillans I. M., and Cassidy W. A. 1983. Catch a falling star: Meteorites on old ice. *Science* 222:55–57.

Wlotzka F. 1993. A weathering scale for the ordinary chondrites (abstract). *Meteoritics* 28:460.

APPENDIX 1. SHIELDING CORRECTED TERRESTRIAL AGES

The ^{36}Cl/^{10}Be-^{10}Be Method

The ^{36}Cl/^{10}Be age is determined using the following correlation for the ^{36}Cl/^{10}Be ratio versus ^{10}Be concentration at saturation:

$$^{36}\text{Cl}/^{10}\text{Be} = 6.01 - 0.28 \times [^{10}\text{Be}] - 0.009 \times [^{10}\text{Be}]^2 \quad \text{(A1)}$$

This correlation is a slight modification of the one given in Lavielle et al. (1999), since we included results for fifteen metal samples of the Gold Basin L-chondrite shower (Welten et al. 2003). The ^{36}Cl/^{10}Be method is only reliable if both ^{36}Cl and ^{10}Be were saturated at the time of fall, i.e., for meteorites with CRE ages >10 Myr. For meteorites with CRE ages <10 Myr, the ^{10}Be concentration can be corrected for undersaturation if the exposure age is known from independent (noble gas) measurements. Corrections are <10% for CRE ages >5 Myr, but lead to increasing uncertainties in the ^{36}Cl/^{10}Be age for shorter CRE ages. The high ^{26}Al/^{10}Be ratio of 0.99 ± 0.03 in FRO 99031 indicates a CRE age of ~2 Myr. The correction for undersaturation of ^{10}Be by 33–48% (assuming an uncertainty of 20% in the CRE age) leads to an uncertainy of >60 kyr in the ^{36}Cl/^{10}Be age. We therefore did not use the ^{36}Cl/^{10}Be method for meteorites with ^{26}Al/^{10}Be ratios >0.77, i.e., with estimated exposure ages of <6–7 Myr. For H chondrites believed to be paired with FRO 90174, we assumed a CRE age of 7.2 Myr (Welten et al. 2001).

The ^{41}Ca/^{36}Cl-^{36}Cl method. Due to the shorter half-life of ^{41}Ca (relative to ^{36}Cl), the ^{41}Ca/^{36}Cl ratio decreases more rapidly with terrestrial age than the ^{36}Cl/^{10}Be ratio. In addition, due to the shorter half-life of ^{36}Cl (relative to ^{10}Be), the ^{41}Ca/^{36}Cl ratio is less dependent on the CRE history of a meteorite. Since the FRO samples studied in this work all have CRE ages >2 Myr, as shown by their ^{26}Al/^{10}Be ratios, they were saturated in ^{41}Ca and ^{36}Cl at the time of fall. The ^{41}Ca/^{36}Cl age is determined using the following correlation for the ^{41}Ca/^{36}Cl activity ratio (at saturation):

$$^{41}\text{Ca}/^{36}\text{Cl} = 1.25 - 0.003 \times [^{36}\text{Cl}] - 0.0006 \times [^{36}\text{Cl}]^2 \quad \text{(A2)}$$

This correlation yields ^{41}Ca/^{36}Cl ratios (at saturation) of 0.90–1.02 for the least shielded samples and of 1.09–1.16 for the most shielded samples (members of the FRO 90174 shower). The average ^{41}Ca/^{36}Cl ratio of 1.05 ± 0.08 agrees with the measured average of 1.06 ± 0.13 which was previously found for a wide range of shielding conditions (Nishiizumi and

Caffee 1998). Typical uncertainties in the $^{41}Ca/^{36}Cl$ ages are 15–25 kyr, whereas those in the $^{36}Cl/^{10}Be$ ages are 25–35 kyr. For meteorites older than 40 kyr, the average ages of the two ages are given in Table 3.

APPENDIX 2. TRAPPED AND COSMOGENIC NOBLE GAS COMPONENTS

Neon

The measured $^{20}Ne/^{22}Ne$ ratios of 0.84–0.90 are very close to the cosmogenic ratio of 0.82–0.84, indicating that the samples contain only very small amounts of atmospheric Ne, which has a $^{20}Ne/^{22}Ne$ ratio of 9.8. Corrections for atmospheric ^{21}Ne are therefore negligible, whereas those for atmospheric ^{22}Ne are <1%. Cosmogenic $^{22}Ne/^{21}Ne$ ratios in FRO 93002, 93054, and 93009 are <1.08, indicating high shielding conditions for these three meteorites.

Argon

The measured $^{36}Ar/^{38}Ar$ ratios of 1.4–3.6 are much higher than the cosmogenic ratio of 0.67, indicating that the meteorites contain a significant component of trapped Ar (atmospheric or primordial), which has a $^{36}Ar/^{38}Ar$ ratio of ~5.32. The amount of trapped (presumably atmospheric) ^{36}Ar is especially high (~3.7×10^{-8} cm^3 STP/g) for FRO 93009, the most weathered meteorite. This suggests that atmospheric Ar is trapped in the Fe,Ni weathering products, as proposed by Scherer et al. (1994). Corrections for trapped Ne and Ar yield cosmogenic $^{21}Ne/^{38}Ar$ ratios of ~13.6 for FRO 93009 and of 9–10 for the other three meteorites. These $^{21}Ne/^{38}Ar$ ratios, especially in FRO 93009, are significantly higher than typical ratios of 7–9 as observed in medium-sized chondrite falls. Although some of the cosmogenic ^{38}Ar may have been lost from the metal due to weathering, it is also possible that we overcorrected for trapped Ar, assuming that all of the "excess" (nonspallogenic) ^{36}Ar is trapped, while instead some of this ^{36}Ar may be due to decay of neutron-capture ^{36}Cl, as was shown for some of the FRO samples as well as for Chico and Gold Basin (Bogard et al. 1995; Welten et al. 2001, 2003). This explanation is especially likely for FRO 93009, which contains a significant contribution of neutron-capture ^{36}Cl, as judged from the ^{36}Cl concentration of 59 ± 3 dpm/kg[Fe +8Ca + 16K] at the time of fall (Table 4).

APPENDIX 3. SHIELDING CORRECTED CRE AGES

After correction for the trapped components, we calculated shielding-corrected CRE ages from the concentrations of cosmogenic ^3He, ^{21}Ne, and ^{38}Ar. For FRO 93005 we used the ^3He and ^{21}Ne production rates of Eugster (1988) and the ^{38}Ar production rates of Schultz et al. (1991). This yields a consistent CRE age of 10 ± 1 Myr (Table 5).

The other three meteorites studied all have $^{22}Ne/^{21}Ne$ ratios below 1.08. It is well known that for these low ratios, which indicate high shielding, the Eugster shielding formalism will overestimate production rates (e.g., Graf et al. 1990; Leya et al. 2000). Assuming maximum production rates (in units of 10^{-8} cm^3 STP/g/Myr) of 0.350 for H- and 0.375 for L chondrites (Graf et al. 1990; Leya et al. 2000) we calculate minimum ^{21}Ne ages of ~5 Myr for FRO 93002/93054 and ~14 Myr for FRO 93009. For FRO 93009, we also calculated the CRE age using the $^{10}Be/^{21}Ne$ and $^{26}Al/^{21}Ne$ methods, which use ^{10}Be and ^{26}Al as internal shielding corrections for the production rate of ^{21}Ne (Graf et al. 1990). Using production rate ratios of 0.132 for $^{10}Be/^{21}Ne$ and 0.37 for $^{26}Al/^{21}Ne$ (Welten et al. 2004), the measured ratios (corrected for radioactive decay of ^{10}Be and ^{26}Al during terrestrial residence) correspond to a $^{10}Be/^{21}Ne$ age of 17 ± 2 Myr and a $^{26}Al/^{21}Ne$ age of 15 ± 2 Myr. We thus adopted a CRE age of 16 ± 2 Myr, derived using the $^{10}Be/^{21}Ne$ and $^{26}Al/^{21}Ne$ methods. This age coincides with the 15 Myr peak in the exposure age distribution of L chondrites, which is most pronounced for L chondrites with low concentrations of radiogenic gases (Marti and Graf 1992). Assuming a $^4He/^3He$ ratio of 6.1 ± 0.3 for cosmogenic He (Alexeev 1998), FRO 93009 yields a radiogenic ^4He concentration of (1.5–1.6) × 10^{-6} cm^3 STP/g, which corresponds to an U,Th-He age of ~600 Myr. Due to the large contribution of atmospheric Ar, the concentration of radiogenic ^{40}Ar is difficult to determine, but is probably <1.0×10^{-6} cm^3 STP/g, corresponding to a K-Ar age of <500 Myr. We thus conclude that FRO 93009 is a member of the L-chondrite group of "poor Ar retainers," that were ejected from their parent body ~15 Myr ago.

The cosmogenic and radiogenic noble gas concentrations in FRO 93002 and 93054 provide strong evidence that these two H6 chondrites are paired with the FRO 90001 group. We concluded previously that FRO 90001 had a preatmospheric radius of <30 cm during the last ~1 Myr, but was exposed under high shielding conditions during most of its exposure history (Welten et al. 2001). The concentrations of cosmogenic ^3He and radiogenic ^4He in six members of this pairing group are very low and show a strong correlation, indicating that these meteorites were degassed in a single event, most likely the recent breakup event ~1 Myr ago. Based on the $^{10}Be/^{21}Ne$ and $^{26}Al/^{21}Ne$ exposure age methods, we previously showed that FRO 90001 probably belongs to the large peak at ~7 Ma in the exposure age histogram of H chondrites (e. g., Graf and Marti 1995). Since FRO 93002 and 93054 show similar cosmogenic noble gas concentrations and similar shielding conditions as other members of the FRO 90001 pairing group, we thus conclude that they have the same CRE age of 7–8 Myr (Table 5).